Estimation of central venous pressure using the ratio of short: long diameter from cross sectional images of the inferior vena cava

Yoshihiro Seo, MD, PhD *, Noriko Iida, BA†, Masayoshi Yamamoto, MD, PhD *, Tomoko Machino-Ohtsuka, MD, PhD *, Tomoko Ishizu, MD, PhD *, and Kazutaka Aonuma MD, PhD *

*Cardiovascular Division, Faculty of Medicine, University of Tsukuba, †Clinical Laboratory, University of Tsukuba Hospital, Tsukuba, Japan

Funding sources: None

Disclosures: None

Address for correspondence: Yoshihiro Seo, MD

Cardiovascular Division, Faculty of Medicine, University of Tsukuba

1-1-1 Tennodai, Tsukuba 305-8575, JAPAN

Phone: +81-298-53-3143

Fax: +81-298-53-3143

E-mail: yo-seo@md.tsukuba.ac.jp

Abstract

Background. The long-axis images of the inferior vena cava (IVC) have limitations as the surrogate of IVC morphology in grading of central venous pressure (CVP) by 2-dimensional echocardiography (2DE), because of the various cross-sectional morphologies and its translational motion by sniffing. On the basis of the relationship between venous pressure and compliance, we hypothesized that the cross-sectional morphology of the IVC, which was obtained by 3-dimensional echocardiography (3DE), might estimate CVP more accurately compared to standard grading by 2DE.

Methods. Consecutive 60 patients who underwent right heart catheterization studies were prospectively enrolled. Echocardiography was performed within 24 hours before catheterization. From 3D datasets, a cross-section of the IVC was determined that was perpendicular to the long-axis reference of the IVC. Short diameter (SD), long diameter (LD), ratio of SD to LD (S/L) as the sphericity index, and area were measured on this cross-section IVC image.

Results. The CVP correlated moderately with SD ($r=0.69$, $p<0.001$), strongly with S/L ($r=0.75$, $p<0.001$), and modestly with area ($r=0.47$, $p<0.001$) but not with LD ($r=0.24$, $p=0.17$). The largest area under the curve by ROC analyses to detect CVP ≥10 mmHg was

0.98 ($p<0.001$, 95% CI 0.97-1.0) for S/L, 0.83 for SD ($p<0.001$, 95% CI 0.74-0.94), and 0.70 for area ($p=0.02$, 95% CI 0.56-0.84). If a cut-off value of 0.69 for S/L was used, the sensitivity, specificity, and accuracy to detect CVP ≥10 mmHg were 0.94, 0.95, and 0.95, and CVP grading by 2DE were 0.59, 0.98, and 0.85, respectively. Estimations of CVP were more accurately reclassified using S/L rather than grading by 2DE (net reclassification improvement 0.38, 95% CI 0.31-0.44, $p<0.001$).

Conclusions S/L of IVC cross-section measured by 3DE may be a reliable parameter to estimate CVP compared to standard grading by 2DE.

Key words: central venous pressure; 3-dimensional echocardiography; Inferior vena cava; heart failure

Abbreviations

Area = area of the cross-section

CVP = central venous pressure

HF = heart failure

IVC = inferior vena cava

LD = long diameter

LV = left ventricular

SD = short diameter

S/L = the ratio of short diameter to long diameter

TR = tricuspid regurgitation

2DE = 2-dimensional echocardiography

3DE = 3-dimensional echocardiography

INTRODUCTION

Interest in right-sided heart failure (HF) has been increasing in the management of left-sided HF.[1-3] Because volume overload of the venous vascular bed is the cause of systemic congestion in right-sided HF, central venous pressure (CVP) is used as a surrogate of the intravascular volume status.[4,5] In addition, CVP is the indicator of filling pressure. CVP is not only a simple hemodynamic parameter to measure, but it is also known as a determinate of clinical outcome in patients with various cardiac diseases.[6-9] Peripheral congestion, in particular, renal congestion caused by increased CVP, also has been focused on as having a central role in cardio-renal syndrome in HF.[7,10] Thus, as the significance of CVP assessment has been increasing, echocardiography is being widely used to estimate CVP levels in the clinical setting because of its noninvasiveness. The current guideline recommends estimation of the CVP by using a combination of the inferior vena cava (IVC) diameter and collapse rate of the IVC by the sniff maneouver.[11] However, findings from major studies evaluating the correlation between IVC and CVP are controversial. [12-14] Thus, we hypothesized that the long-axis images of the IVC might have limitations as the surrogate of IVC morphology because the IVC is often elliptical, curved, and flat in cross-section. In addition, translational motion of the IVC caused by sniffing might be a limitation in assessing the collapse rate

accurately. Based on the relationship between venous pressure and venous compliance, the cross-sectional morphology of the IVC might be useful to estimate CVP.[14-17] In addition, 3-dimensional echocardiography (3DE) might be helpful in assessing the correct cross-sectional morphology of the IVC because of limitations of 2-dimensional echocardiography (2DE). Therefore, we aimed to investigate the accuracy of CVP estimation by using cross-sectional morphology parameters of the IVC obtained by 3DE compared to the general grading of CVP by 2DE.

Methods

Study design. To assess the associations between IVC parameters and CVP, we prospectively enrolled consecutive 60 patients who underwent right heart catheterization studies for the assessment of cardiovascular diseases at the University of Tsukuba Hospital from April 2014 to May 2016. The indications of right heart catheterization studies were as follows; hemodynamic evaluations for decision-making of interventions in valvular diseases or congenital heart diseases, to diagnose a cause of heart failure with or without right ventricular biopsy, to assess the therapeutic effects in heart failure or pulmonary

hypertensions, and to diagnose the cause of pulmonary hypertensions with or without pulmonary artery angiography.

Echocardiographic studies were performed within 24 hours before catheterization. The hospital ethics committee approved the research protocol, and informed consent was obtained from each subject. This study complied with the Declaration of Helsinki.

Echocardiography. Comprehensive transthoracic echocardiographic examinations were performed with a Vivid E9 system (GE Healthcare, Horton, Norway) with a variable-frequency 2.5-5 MHz sector transducer, and each echocardiographic parameter was measured and evaluated according to the American Society of Echocardiography (ASE) guidelines.[18,19] Left ventricular (LV) volume, LV ejection fraction, pulsed Doppler transmitral flow profiles, and tissue Doppler study by spectral Doppler method on the mitral annulus were assessed. Right ventricular function was assessed by tricuspid annular plane systolic excursion and fractional area change ratio. In patients with tricuspid regurgitation (TR), peak pressure gradients between the right ventricle and right atrium were measured, and the degree of TR was assessed as the ratio of the maximal TR jet area to the corresponding right atrial

area: <20% was defined as mild TR, 20–40% as moderate TR, and ≥40% as severe TR. The velocity of flow in the hepatic veins was recorded from the subcostal window, and the hepatic systolic (S) and diastolic flow (D) velocities and the S/D ratio were measured. With the patient in the supine position, IVC diameters were measured in the subcostal view at 1.0 to 2.0 cm from the junction with the right atrium.[11] IVC diameters were measured as the inner-inner dimension of the IVC. The maximum diameter of the IVC and the percentage decrease in the diameter during inspiration were measured. Based on the ASE guidelines, the CVP was estimated using 3 grades consisting of 3, 8, and 15 mmHg.

Three-dimensional echocardiography. 3DE datasets consisting of 4 consecutive cardiac cycles at end-expiration were obtained using a subxiphoid approach with the patient in the supine position. In patients with atrial fibrillation, a single-beat full-volume 3DE dataset was acquired. From these 3D datasets, a cross-section of the IVC was determined that was perpendicular to the long-axis reference of the IVC at 0.5 to 3 cm from the right atrium by offline analysis using commercially available software (EchoPAC PC, Ver. 104.3.0; GE Healthcare) (Figure 1). On the cross-section image of the IVC, the short diameter (SD), long diameter (LD), area of the cross-section (Area), and indexed Area calculated as IVC area / body surface area were measured. The line for the LD measurement was determined by

visual evaluation, and corrected manually to obtain the maximum length. In addition, SD was measured on the longest line perpendicular to the direction of the line used to measure LD. The ratio of SD to LD (S/L ratio) was calculated.

Cardiac catheterization. Right heart catheterization was performed via a femoral or jugular vein approach. A 7Fr balloon-tipped pulmonary artery catheter (Swan-Ganz, Baxter Healthcare, Irvine, CA) was used to measure right atrial pressure, right ventricular pressure, pulmonary artery pressure, and pulmonary capillary wedge pressure. All pressure data were measured at end-expiration, and the reported values represent the average of 5-10 cardiac cycles. The cardiac index was measured by the Fick method.

Reproducibility. Two observers independently assessed the 3D-IVC parameters in 20 patients. To test intra-observer variability, a single observer analyzed the data twice on occasions separated by 1 month. To test inter-observer variability, a second observer analyzed the data without knowledge of the first observer’s measurements. Reproducibility was assessed as the mean percent error (absolute difference divided by the mean of the two observations).

Statistical analysis. Results are expressed as number (%) or as mean ± SD. Correlations between CVP and 3D-IVC parameters were evaluated by Pearson's correlation coefficient. Correlations between CVP and CVP grading by 2DE were assessed by Spearman's rank correlation. We assessed the performance of the 3D-IVC parameters to predict a CVP ≥10 mmHg using the area under the curve (AUC) of the receiver operating characteristic (ROC) curve.

Agreements of the diagnosis of CVP ≥10 mmHg between the catheterization data and the S/L ratio, and the ASE guideline-based CVP = 15 mmHg were assessed with Cohen's κ coefficients.

The incremental effects of the S/L ratio to predict a CVP ≥10 mmHg were assessed by net reclassification improvement (NRI),[20] which was calculated by the following formula:

NRI = [P(up | D = 1) - P(down | D = 1)] - [P(up | D = 0) - P(down | D = 0)],

where P is the proportion of patients, upward movement (up) is defined as a change into a higher probability of CVP ≥10 mmHg category based on the S/L ratio, and downward movement (down) is defined as a change in the opposite direction. D denotes the response classification, with CVP ≥10 mmHg = 1 and CVP <10 mmHg = 0.

A p-value <0.05 was considered to indicate statistical significance. All calculations were performed with SPSS ver. 22 (SPSS Inc., Chicago, IL). In addition, comparisons of AUC were performed with Analyse-it (Analyse-it Software, Ltd., Leeds, UK).

Results

Adequate 2D- and 3D-IVC images were obtained in all patients. Clinical characteristics and echocardiographic parameters are summarized in Table 1.

In the comparisons of CVP grades, CVP at the grade of 3 mmHg did not differ from those of 8 mmHg, but CVP at the grade of 15 mmHg was significantly higher than those at the other grades (Figure 2).

Representative images of IVC cross-sections are shown in Figure 3. The CVP correlated moderately with SD ($r=0.69$, $p<0.001$), and strongly with S/L ($r=0.75$, $p<0.001$), but not with LD ($r=0.24$, $p=0.17$) (Figure 4-a). Area showed the modest correlation with CVP ($r=0.47$, $p<0.001$), and indexed Area also showed the similar correlation ($r=0.47$, $p<0.001$) (Figure 4-b). The largest AUC by ROC analyses to detect a CVP ≥10 mmHg was 0.98 ($p<0.001$, 95% confidence interval [CI] 0.97-1.0) for S/L followed by 0.83 for SD ($p<0.001$, 95% CI 0.74-0.94) and 0.70 for Area ($p=0.02$, 95% CI 0.56-0.84) (Figure 5). If a cut-off value of 0.69

for S/L was used, the sensitivity, specificity, and accuracy to detect a CVP ≥10 mmHg were 0.94, 0.95, and 0.95, whereas those for CVP grading by 2DE were 0.59, 0.98, and 0.85, respectively. In addition, the kappa statistic of S/L was excellent (0.82), and that of CVP grading by 2DE was fair (0.5). The reclassification table for the CVP example is shown in Table 2. Using S/L, estimations of CVP were more accurately reclassified from grading by 2DE as the NRI was 0.38 (95% CI 0.31-0.44,($p<0.001$). In particular, the improvements were observed in patients with a CVP ≥10 mmHg.

In terms of reproducibility, the intra- and inter-observer variability of LD, SD, S/L, and Area were LD: 2.6 ± 1.9 and 4.3 ± 3.9%; SD: 1.7 ± 1.1 and 5.1 ± 3.3%; S/L: 2.9 ± 1.8 and 4.3 ± 2.1%; and Area: 4.5 ± 4.9 and 7.8 ± 4.8%, respectively.

Discussion

The present study showed that S/L of the IVC accurately predicted a CVP ≥10 mmHg. To our knowledge, this is the first study in which 3DE IVC images have been used to estimate CVP.

S/L of IVC. The S/L of the IVC cross-section was the best predictor of increased CVP. This finding was attributed to the feature of venous compliance to changes in pressure. [15-17] In the lower range of CVP, the IVC has the largest compliance, showing small increases in CVP

despite large changes in intravascular volume (Figure 5). In contrast, at the relatively higher range of CVP, the IVC cross-section shows a more rounded shape, corresponding to a higher S/L. Based on the association between CVP and IVC compliance in this study, an S/L of around 0.7 may correspond to a value of 10 mmHg. A previous study of peripheral veins showed that venous compliance was rapidly reduced at around 10 mmHg of venous pressure. Although the association between CVP and IVC compliance has not been well studied, our data suggest the same pathophysiology as that of peripheral veins. However, once the IVC has obtained a round shape, with further increases in CVP, the change in S/L is slight and may be less sensitive at the upper range of CVP, which means the S/L may be not helpful in assessing CVP >15 mmHg as shown in Figure 4.

Interestingly, cross-sectional IVC areas showed a modest correlation with CVP. Body surface area and height have significant but only weak correlations with cross-sectional areas ($r = 0.31$, $p = 0.02$, $r = 0.33$, $p = 0.01$, respectively), which may be associated with the modest correlation of indexed IVC area with CVP. Therefore, other mechanisms that affect vascular properties are assumed. In peripheral veins, vascular spasm is a well-known phenomenon that is caused by activation of the autonomic nerves.[17, 21] Such vasospastic phenomenon might also occur in the IVC, in particular in patients with heart failure, because neurohormonal

factors are activated in a decompensated state. As shown in Figure 3, despite a smaller cross-sectional dimension, the CVP was higher in a patient with a higher S/L (Case C vs. Case D). Therefore, S/L is superior to ~~simple~~ the cross-sectional area to estimate CVP levels.

CVP estimations by one-directional dimension. The 3D LD did not correlate with CVP despite the 3D SD showing a significant correlation with CVP. If a change in the cross-section caused by blood volume and pressure is considered, the change in the 3D SD is more dynamic than that in the 3D LD because S/L is dependent on 3D SD but not on LD. In addition, the 3D LD might rather shorten when changing from a collapsed shape to a round shape. These factors make the 3D LD less sensitive for determining changes in CVP. Positions to measure IVC may affect the diameters. Nakao et al. [22] reported that IVC diameters were largest in right lateral position, intermediate in supine position, and smallest in left lateral position. In addition, IVC diameters measured in left lateral position showed more strong correlations with CVP compared to those in supine position that we used. Since we did not compare the differences between positions, we might not conclude the inferiority of CVP estimation by 2D method compared to our 3D method. In contrast, this study found that the IVC shape in the short-axis view was round in patients with high CVP independent of

positions. The finding supports our findings and suggests advantages of the S/L of the cross-sectional IVC by 3DE.

Clinical implications. Although various advantages of 3DE have been introduced for examinations of the heart, the technique remains unfamiliar in the clinical setting because of technical complications in its use. In contrast, the conditions for 3D imaging of the IVC are better than those for the heart because of easily addressed echo windows and the reduced movement of the IVC as opposed to the dynamic motion of the heart. In addition, the reproducibility with 3DE was acceptable for clinical use. Therefore, 3DE may be a feasible technique that shows better accuracy for the estimation of the CVP level. As compared with the standard grading by 2DE, our method may contribute to the more accurate screening of higher CVPs as shown in Table 2.

Limitations. Because of 3DE nature, 3DE has poorer spatial and temporal resolutions compared to 2D method. In a single-beat full-volume 3DE dataset, the volume rate was from 10 to 15 volume/sec, which might affect the accuracy to obtain IVC morphological data. Furthermore, catheterization and echocardiographic studies were not performed

simultaneously, which might also affect the results. In addition, our study was a single-center study with a small number of patients and did not have another cohort to validate our results. Therefore, we emphasize the cutoff of 3DE is only a preliminary value and to need a prospective study, in which both catheterization and echocardiography are performed simultaneously, in order to validate our findings. In addition, large-scale prospective studies will be needed to confirm the clinical usefulness of our method.

Conclusions

The ratio of short diameter to long diameter of the IVC cross-section obtained by 3DE may be a reliable parameter to estimate CVP compared to standard 2DE parameters and other 3DE parameters.

References

1. Kjaergaard J, Akkan D, Iversen KK, Køber L, Torp-Pedersen C, Hassager C. Right ventricular dysfunction as an independent predictor of short- and long-term mortality in patients with heart failure. Eur J Heart Fail 2007;9:610–6.

2. Meyer P, Filippatos GS, Ahmed MI, Iskandrian AE, Bittner V, Perry GJ et al. Effects of right ventricular ejection fraction on outcomes in chronic systolic heart failure. Circulation 2010;121:252–8.

3. Mohammed SF, Hussain I, AbouEzzeddine OF, Takahama H, Kwon SH, Forfia P et al. Right ventricular function in heart failure with preserved ejection fraction: a community-based study. Circulation 2014;130:2310–20.

4. Central venous pressure: an indicator of circulatory hemodynamics. In: Mohrman DE, Heller LJ, editors. Lange cardiovascular physiology. 6th ed. New York: McGraw-Hill; 2006.

5. Mark JB, Slaughter TF. Cardiovascular monitoring. In: Miller RD, editor. Miller's anesthesia. 6th ed. Orlando, FL: Churchill Livingston; 2005

6. Drazner MH, Rame JE, Stevenson LW, Dries DL. Prognostic importance of elevated jugular venous pressure and a third heart sound in patients with heart failure. N Engl J Med 2001;345:574–81.

7. Damman K, van Deursen VM, Navis G, Voors AA, van Veldhuisen DJ, Hillege HL. Increased central venous pressure is associated with impaired renal function and mortality in a broad spectrum of patients with cardiovascular disease. J Am Coll Cardiol 2009;53:582–8.

8. Pellicori P, Carubelli V, Zhang J, Castiello T, Sherwi N, Clark AL et al. IVC diameter in patients with chronic heart failure: relationships and prognostic significance. JACC Cardiovasc Imaging 2013;6:16–28.

9. Benza RL, Gomberg-Maitland M, Miller DP, Frost A, Frantz RP, Foreman AJ et al. The REVEAL Registry risk score calculator in patients newly diagnosed with pulmonary arterial hypertension. Chest 2012;141:354–62.

10. Mullens W, Abrahams Z, Francis GS, Sokos G, Taylor DO, Starling RC et al. Importance of venous congestion for worsening of renal function in advanced decompensated heart failure. J Am Coll Cardiol 2009;53:589–96.

11. Rudski LG, Lai WW, Afialo J, Hua L, Handschumacher MD, Chandrasekaran K et al. Guidelines for the echocardiographic assessment of the right heart in adults: a report from the American Society of Echocardiography endorsed by the European Association of Echocardiography, a registered branch of the European Society of Cardiology, and the Canadian Society of Echocardiography. J Am Soc Echocardiogr 2010;23:685–713

12. Brennan JM, Blair JE, Goonewardena S, Ronan A, Shah D, Vasaiwala S, et al. Reappraisal of the use of inferior vena cava for estimating right atrial pressure. J Am Soc Echocardiogr 2007;20:857-61.

13. Beigel R, Cercek B, Luo H, Siegel RJ. Noninvasive evaluation of right atrial pressure. J Am Soc Echocardiogr 2013;26:1033–42.

14. Lee SL, Daimon M, Kawata T, Kohro T, Kimura K, Nakao T et al. Estimation of right atrial pressure on inferior vena cava ultrasound in Asian patients. Circ J 2014;78:962–6.

15. Rothe CF. Venous System: Physiology of the Capacitance Vessels. Handbook of Physiology, The Cardiovascular System, Peripheral Circulation and Organ Blood Flow Published Online: 1 JAN 2011. DOI: 10.1002/cphy.cp020313.

16. Katz AI, Chen Y, Moreno AH. Flow through a collapsible tube. Experimental analysis and mathematical model. Biophys J 1969;9:1261-79.

17. Gelman S. Venous function and central venous pressure: a physiologic story. Anesthesiology 2008;108:735–748.

18. Lang RM, Badano LP, Mor-Avi V, Afilalo J, Armstrong A, Ernande L, et al. Recommendations for cardiac chamber quantification by echocardiography in adults: an update from the American Society of Echocardiography and the European Association of Cardiovascular Imaging. J Am Soc Echocardiogr 2015;28:1-39.

19. Zoghbi WA, Enriquez-Sarano M, Foster E, Grayburn PA, Kraft CD, Levine RA et al. Recommendations for evaluation of the severity of native valvular regurgitation with two-dimensional and Doppler echocardiography. J Am Soc Echocardiogr 2003;16:777–802.

20. Pencina MJ, D'Agostino RB Sr, D'Agostino RB Jr, Vasan RS. Evaluating the added predictive ability of a new biomarker: from area under the ROC curve to reclassification and beyond. Stat Med 2008;27:157–172.

21. Fallick C, Sobotka PA, Dunlap ME. Sympathetically mediated changes in capacitance: redistribution of the venous reservoir as a cause of decompensation.

Circ Heart Fail 2011;4:669–75.

22. Nakao S, Come PC, McKay RG, Ransil BJ. Effects of positional changes on inferior vena caval size and dynamics and correlations with right-sided cardiac pressure. Am J Cardiol 1987;59:125-32.

Figure Legends

Figure 1 Three-dimensional (3D) images and measurements of the inferior vena cava (IVC). Left panel: 3D image of the IVC. The white dashed line is the long-axis reference, and the black line, which is perpendicular to the direction of the long-axis reference, is the cross-section reference line. Middle panel: cross-section image reconstructed from the 3D image of the IVC. Right panel: Measurements on the cross-section image. The blue dashed line is the long diameter, the red dashed line is the short diameter, and the white dashed line defines the cross-sectional area.

Figure 2 Comparisons of central venous pressure (CVP) between the three CVP grades from the guideline. Error bars show average and range of standard deviation. * $p<0.001$, # $p=0.01$ vs. CVP grade of 15 mmHg.

Figure 3 Plotting of representative images of IVC cross-sections based on the correlation between the ratio of SD to LD (S/L) and central venous pressure (CVP).

Figure 4-a Correlations of SD, LD, and S/L with central venous pressure (CVP). The vertical dashed line indicates the optimal cut-off value to detect a CVP of ≥10 mmHg based on receiver operating characteristic analysis of each parameter. The horizontal dashed line indicates a CVP of 10 mmHg.

Figure 4-b Correlations of Area and indexed Area with central venous pressure (CVP). Dashed lines indicate same as Figure 4-a.

Figure 5 Receiver operating characteristic curves to detect a central venous pressure ≥10 mmHg. Area, area of cross-section; LD, long diameter; SD, short diameter; S/L, ratio of SD to LD.

Figure 1

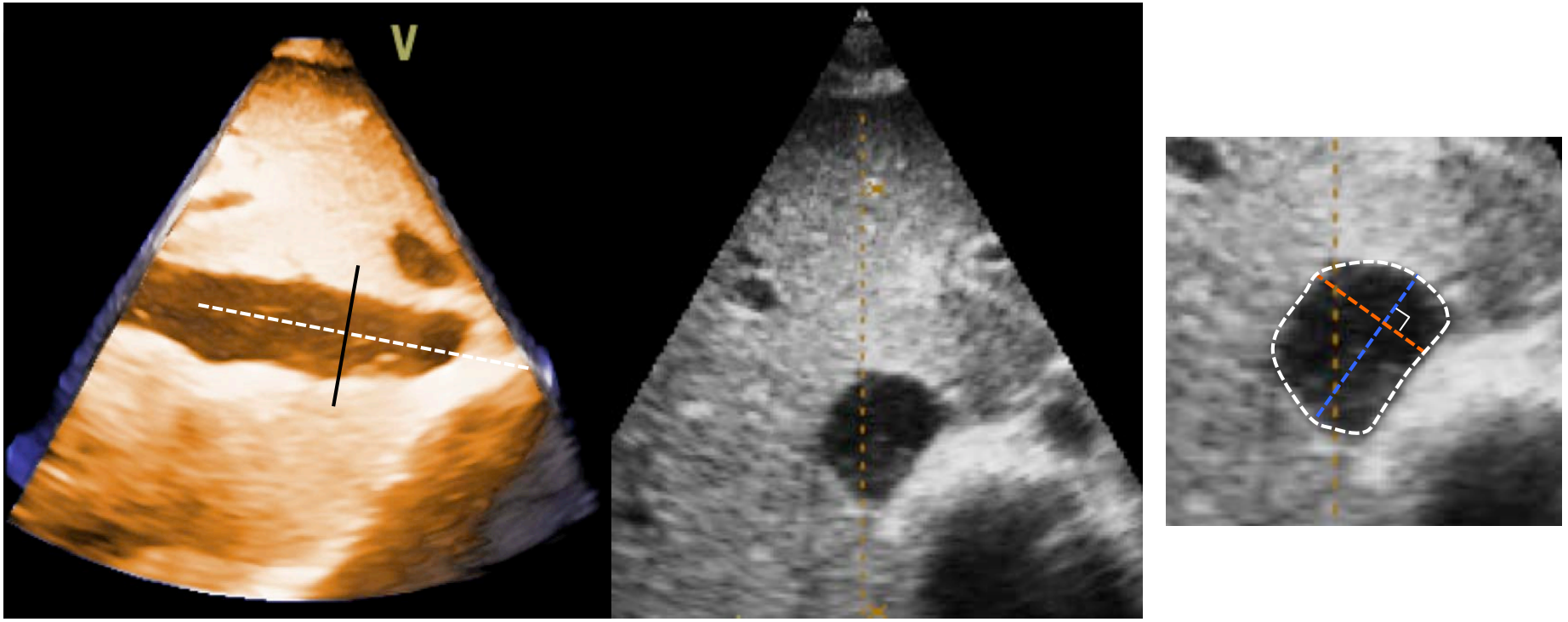

Figure 2

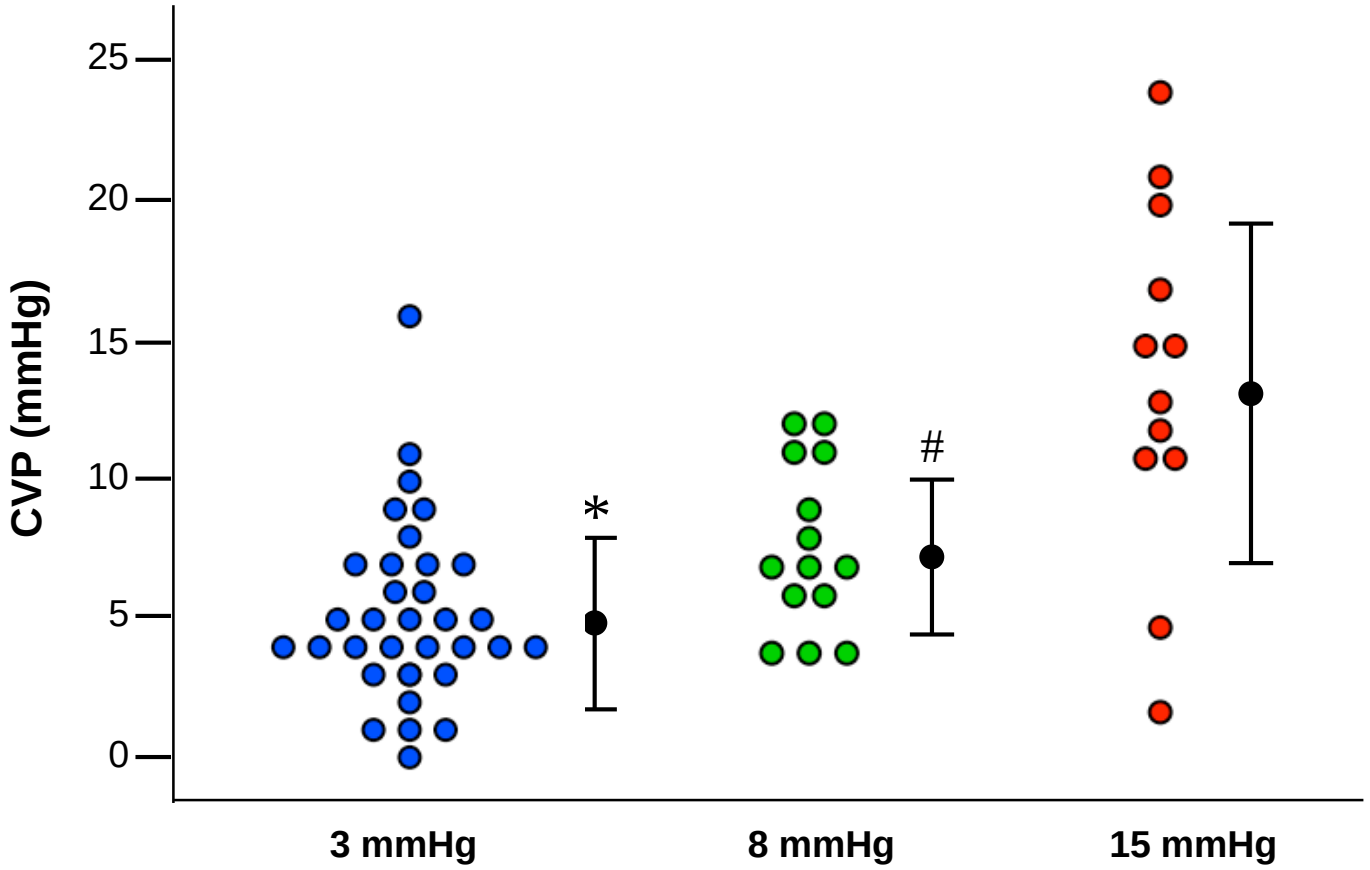

Figure 3

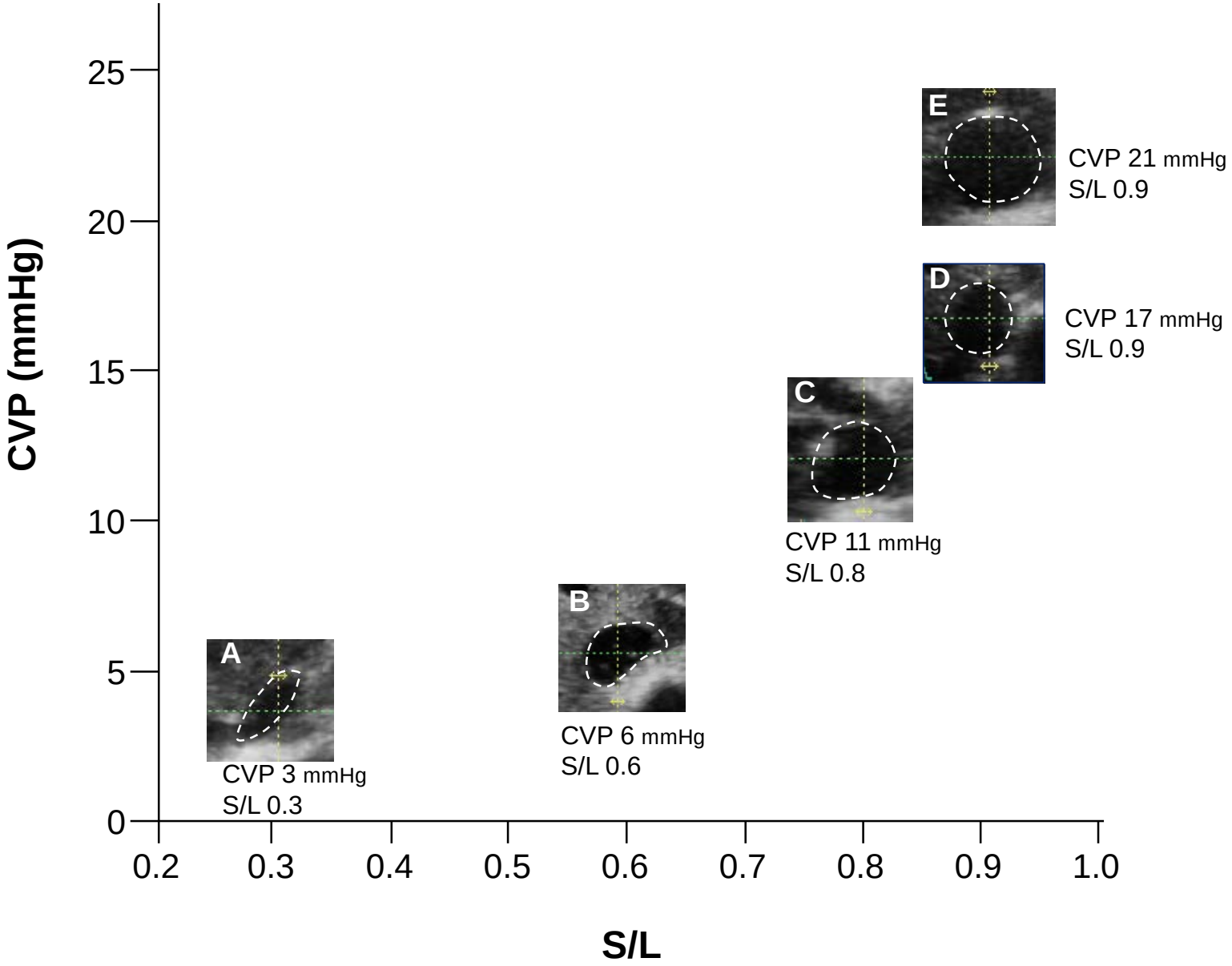
CVP (mmHg)
25
20
15
10
5
0
0.2
0.3
0.4
0.5
0.6
0.7
0.8
0.9
1.0
S/L
A
CVP 3 mmHg
S/L 0.3
B
CVP 6 mmHg
S/L 0.6
C
CVP 11 mmHg
S/L 0.8
D
CVP 17 mmHg
S/L 0.9
E
CVP 21 mmHg
S/L 0.9

Figure 4-a

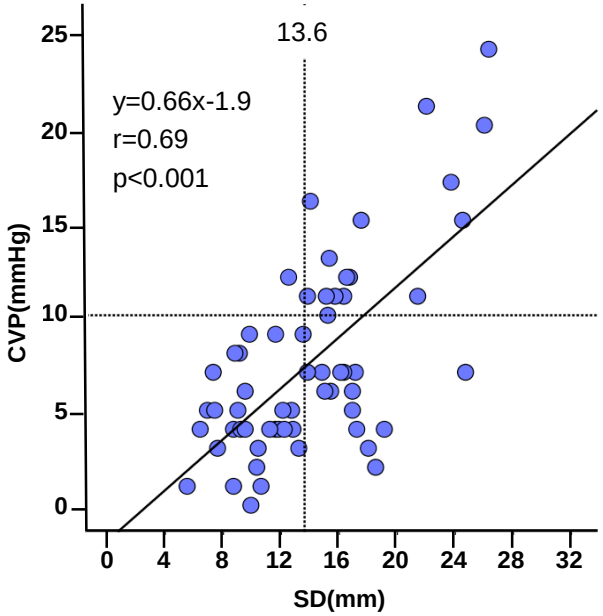
13.6
y=0.66x-1.9
r=0.69
p<0.001
CVP(mmHg)
SD(mm)

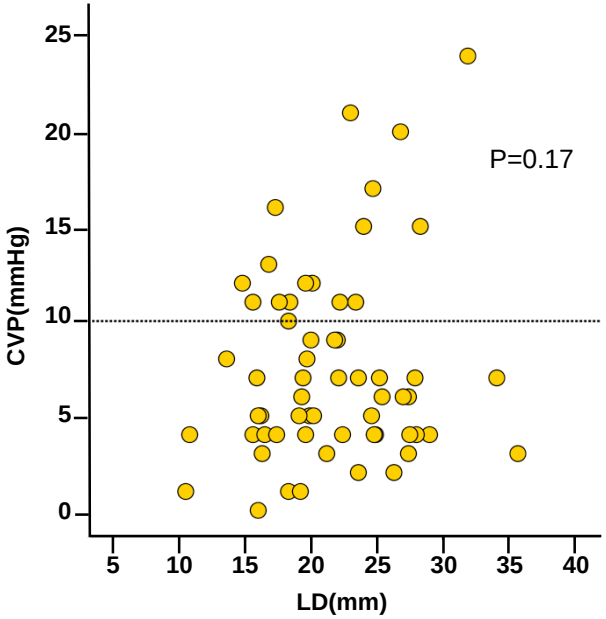
P=0.17
CVP(mmHg)
LD(mm)

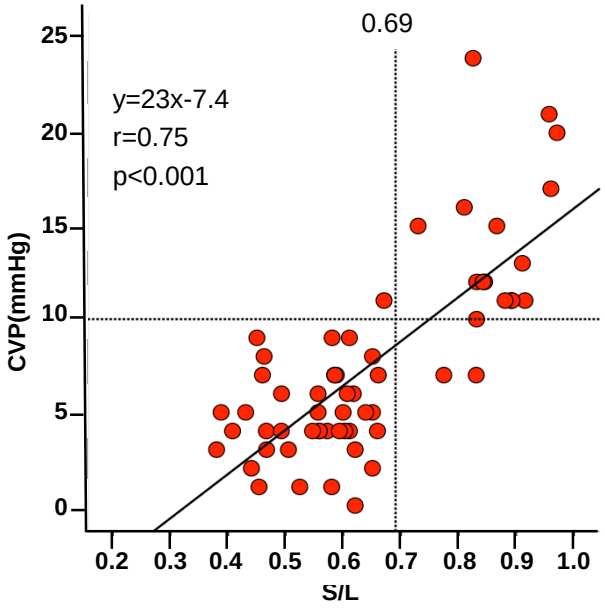
0.69
y=23x-7.4
r=0.75
p<0.001
CVP(mmHg)
S/L

Figure 4-b

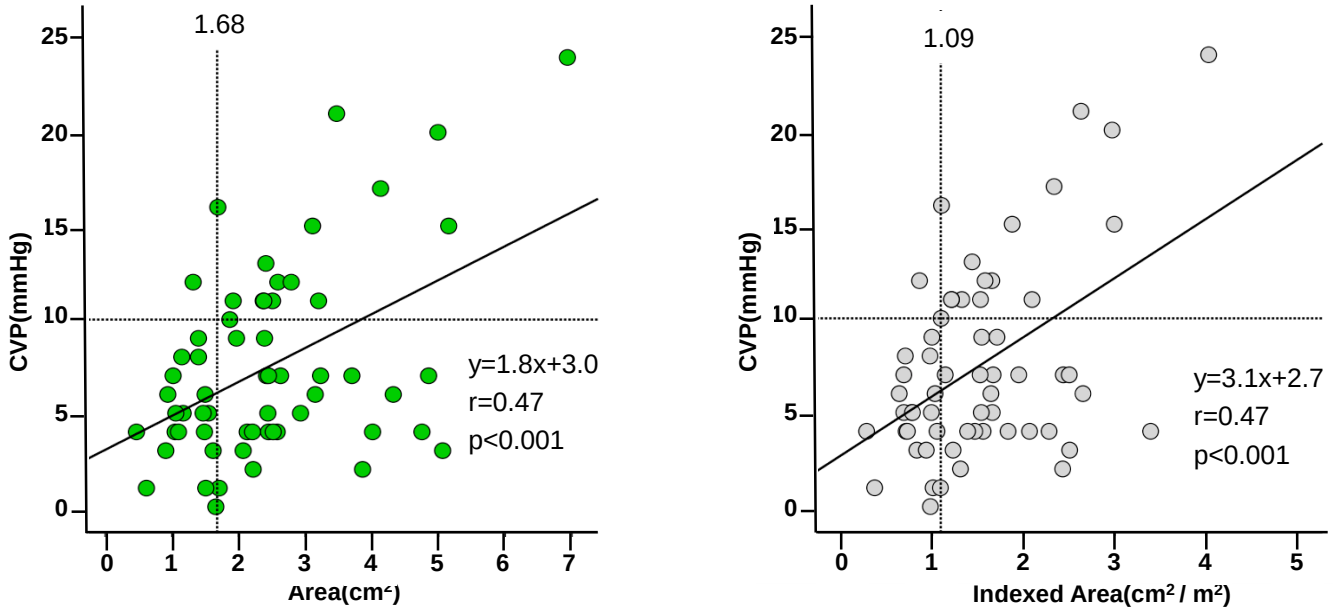
1.68
CVP(mmHg)
Area(cm²)
y=1.8x+3.0
r=0.47
p<0.001
1.09
Indexed Area(cm² / m²)
y=3.1x+2.7
r=0.47
p<0.001

Figure 5